Shape Morphing and Slice Shift Correction in Congenital Heart Defect Model Generation

Pentenga, Puck; Stroh, Ashley; van Genuchten, Wouter; Helbing, Wim A.; Peirlinck, Mathias

Important note
To cite this publication, please use the final published version (if applicable).
Please check the document version above.

Shape Morphing and Slice Shift Correction in Congenital Heart Defect Model Generation

Puck Pentenga[1], Ashley Stroh[2], Wouter van Genuchten[3], Wim A. Helbing[3], and Mathias Peirlinck[1(✉)]

[1] Delft University of Technology, Delft, The Netherlands
mplab-3me@tudelft.nl
[2] Dassault Systemes Simulia Corp., Johnston, RI, USA
[3] Erasmus MC-Sophia Children's Hospital, Rotterdam, The Netherlands

Abstract. Computational heart modeling is a promising approach for improving the prognosis of patients born with congenital heart defects. To create accurate physics-based digital cardiac twins of this population, it is crucial to accurately represent the highly diverse and unique subject-specific heart geometry. In young pediatric patients, this is a challenging endeavor given the lack of high-spatial-resolution imaging data and the risk of slice misalignment. In this study, we set up a multistep shape morphing and slice correction approach to accommodate these challenges and establish a population of biventricular heart models for a variety of healthy, Fallot, and Fontan pediatric patients.

Keywords: Shape Morphing · Congenital Heart Defects · Cardiac digital twins

1 Introduction

Congenital heart defects (CHDs) are one of the most common birth defects, affecting approximately 1% of newborns worldwide. Within this population, approximately 40% of the patients require one or more surgeries during their lifetime. As surgical treatment is seldom curative, many patients with CHD suffer from complications later in life, the most common being heart failure [9]. Heart failure leads to severe debilitating symptoms, drastically reducing the patient's quality of life. Furthermore, it is the most common cause of death in CHD patients worldwide.

Computational heart models offer a promising platform to improve the long-term outlook for this challenging patient population [12]. These models integrate imaging and diagnostic data with physiological and physical principles to provide detailed insights into cardiac function [13,16]. Given the large variability and complexity of CHD anatomical configurations, a computational analysis of CHD cardiac function requires a patient-specific approach [4,8,15,19].

Setting up patient-specific heart models involves geometric reconstruction and meshing based on cardiac imaging data [17]. Within a CHD population,

this is a challenging and cumbersome task. Avoiding harmful radiation in children, magnetic resonance imaging (MRI) is the most suitable technique [2,6]. Unfortunately, MRI in younger children poses significant challenges due to non-compliance with breath-holding and faster heart and respiratory rates [11]. This limits the spatiotemporal resolution of clinically available cardiac MR images in this young population. Deducing detailed three-dimensional models from these images is often time consuming and inconsistent [21]. Shape morphing can be an interesting technique to overcome some of these challenges. This is a technique to convert one three-dimensional geometrical model into another through global and local geometric interpolation techniques. Doing so, we can reconstruct one geometry from another without losing the original topology. Preserving the topology is highly favorable for quantifying individual variations in heart anatomy between patients and for mapping routinely unavailable geometrical details, such as the cardiac myofiber architecture or the Purkinje networks, from one model to another. In this study, we set up a shape morphing framework to construct subject-specific CHD geometries and explore the intrinsic opportunities and challenges this framework entails.

2   Methods

2.1   Cardiac Imaging Data Collection and Segmentation

Anonymized MRI data of seven pediatric patients was collected at the Erasmus University Medical Center. The image data set comprised two healthy female patients aged 8 and 9 years, two male patients with repaired tetralogy of Fallot aged 7 and 8 years, and three male single ventricle patients with Fontan physiology aged 5, 8 and 19. On average, our imaging dataset had a spatial resolution of 1.8–2.0 mm × 1.8–2.1 mm, a temporal resolution of 27–32 ms repetition time 3.41–3.75 ms, echo time 1.31–1.62 ms, flip angle 45 deg, and slice thickness 8 mm and an interslice gap of 1–2 mm. Left and right ventricular contours in the short-axis slices were semiautomatically segmented by a clinician in Medis (Medical Imaging Systems, Leiden, Netherlands), see Fig. 1 - left. The left and right ventricular top contours were segmented on the short axis slices containing the mitral and tricuspid valve respectively.
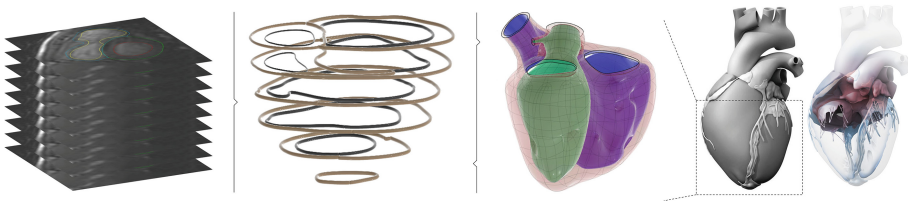

Fig. 1. Inputs to the shape morphing workflow: (left) cardiac image data collection and segmentation contours - (right) high-resolution biventricular CAD geometry deduced from an average 21year-old Caucasian male [24].

2.2   High-Resolution Baseline Model

For our baseline geometry, we make use of a three-dimensional model of the heart of a healthy, 21 year-old, 50th percentile Caucasian U.S. male, created by the Zygote Media Group [24]. This model was deduced from high-resolution MRI data consisting of 0.75 mm thick slices. We imported this geometry in the 3DEX-PERIENCE platform (Dassault Systemes, Rhode Island, USA) and constructed three NURBS multipatch surfaces of the left ventricular endocardium, the right ventricular endocardium, and the biventricular epicardium, respectively, with the Zygote geometry as a reference (see Fig. 1 - right). The left ventricular geometry was further morphed to another patient-specific MRI scan.

2.3   Shape Morphing Workflow

We followed a four-step approach to morph the high resolution baseline geometry to the subject-specific contours: global scaling, global alignment, parametric morphing, and manual morphing (see Fig. 2). In the *global scaling* step, we matched the volumetric dimensions of the left and right ventricles to those of the segmented contours. We updated the dimensions by adjusting the affinity dimensions of the endocardium surfaces, which automatically rescaled the epicardial surface. In the *global alignment* step, we semi-automatically found the best translation and rotation parameters to align the globally scaled reference geometry with the endo- and epicardial constraints. The *parametric morphing* step involved making localized adjustments to the endo- and epicardial surfaces. We adjusted the LV and RV long axis length, septal long axis angle, anterior/posterior long axis angle parameters, and ventricle diameter parameters. In the final *manual morphing* step, we selected control nodes on the LV endocardium, RV endocardium, and epicardium surfaces and made additional localized adjustments to each NURBS surface. Throughout the entire shape morphing workflow, we conducted interference checks to ensure that no surfaces intersected.
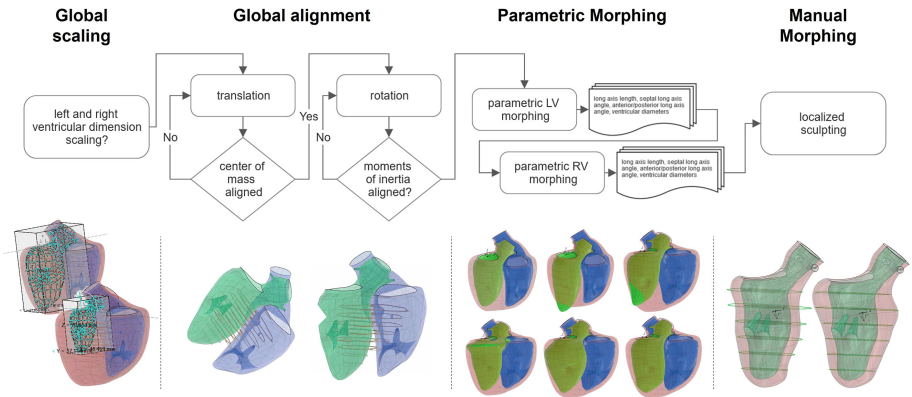

Fig. 2. Shape morphing workflow including a global scaling, global alignment, parametric morphing and manual morphing step.

2.4   Slice Shift Correction

MR imaging can result in both short- and long-axis slice misalignment, also known as slice shift, due to inconsistent breath-holding and/or movement. To address this issue prior to morphing, we proposed two correction approaches. In our first approach, we assumed that the left ventricular *papillary muscles* was an *anatomical straight line* landmark. Following this assumption, we translated all short-axis MR segmentation contours within their respective plane such that the segmented papillary muscles were aligned. In our second approach, we assumed the *center of mass* of each *LV endocardial contour* to be *aligned*. We translated all short-axis MR segmentation contours with respect to their respective LV endocardial centers of mass.

For the patient in our cohort with the slice shift, we qualitatively and quantitatively compared long-axis MR-based segmentation with long-axis slices made from our resulting short-axis-image-morphed geometry. More specifically, we computed the Dice Similarity Coefficient (DSC), which evaluates the overlap between the ground truth (long-axis MR image contours) and long-axis slices of the morphed geometry on a pixel-by-pixel basis [23].

3   Results

3.1   Morphing Accuracy

The final result of the morphing workflow for one of the patients is shown in Fig. 3. For each of the patients, we computed DSC scores that quantified the local match between the clinically segmented short-axis contours and short-axis slices of the final morphed geometries. The respective resulting DSC scores are shown in Table 1. We report DSC scores ranging between 0.830 (best case - patient 7) and 0.681 (worst case - patient 6).

Table 1. Morphing accuracy, expressed in terms of short-axis Dice Similarity Coefficients (DSC).

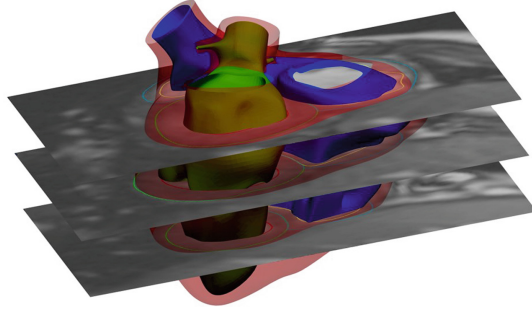| Patient	Sex	Age	DSC
1. Healthy	F	8	0.691 ± 0.155
2. Healthy	F	9	0.750 ± 0.073
3. Tetralogy of Fallot	M	7	0.768 ± 0.040
4. Tetralogy of Fallot	M	8	0.711 ± 0.138
5. Fontan	M	5	0.801 ± 0.138
6. Fontan	M	8	0.681 ± 0.204
7. Fontan	M	19	0.830 ± 0.037

Fig. 3. Final result of shape morphing workflow: a patient-specific Tetralogy of Fallot heart CAD geometry (patient 3).

3.2   Slice Shift Correction

Figure 4 showcases the original slice shift present in Patient 2, and the two different approaches we followed to correct for this misalignment. It can be seen that both approaches tend to restore a more natural ellipsoidal shape for the left ventricle after correction. More specifically, the papillary muscle-based and endocardial center of mass correction approaches amounted to slice shifts of 13.937 ± 3.11 mm and 10.123 ± 4.26 mm respectively.
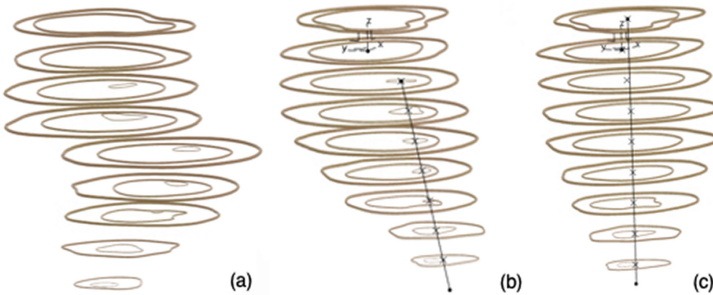
Fig. 4. Slice shift misalignment comparison of correction methods in LV of Patient 2 (healthy heart). Comparison of original data with two correction methods using the center-of-gravity points. (a) Original contours (b) Alignment through papillary muscle (c) Alignment through LV endocardial center of masses.

A qualitative and quantitative validation of this slice shifting approach can be found in Fig. 5. As can be seen, the original model suffered from the slice shift with a long-axis based DSC = 0.747. Both the papillary muscle-based (DSC = 0.916) and LV endocardial center of mass-based (DSC = 0.877) improved the fit to the collected long-axis image slice.

no slice shift correction   **papillary muscle-based slice shift correction**   **LV center of mass-based slice shift correction**
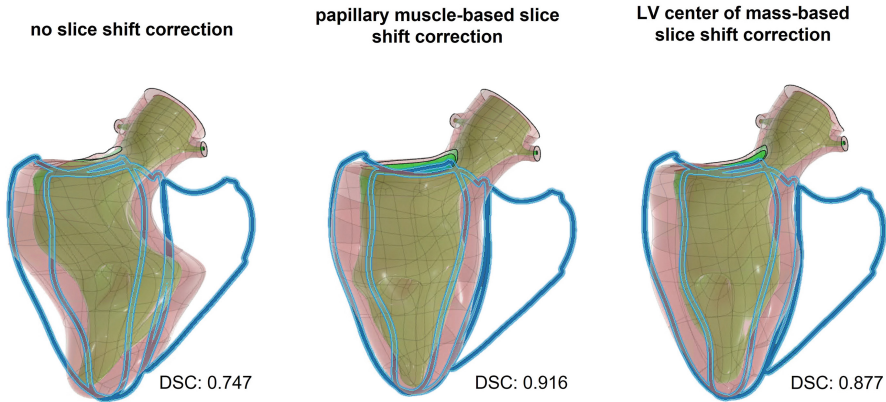
DSC: 0.747   DSC: 0.916   DSC: 0.877

Fig. 5. Qualitative and quantitative validation of our slice shift correction approaches.

4 Discussion

We established and validated a shape morphing framework to develop subject-specific heart models for pediatric patients with complex CHD heart anatomies. Subsequently, we tested two approaches to correct slice shifts, a known problem in pediatric magnetic resonance imaging, both qualitatively and quantitatively.

Shape Morphing Flexibility. We found that our shape morphing workflow provided us with ample flexibility to establish subject-specific heart models while maintaining the original high-fidelity adult human heart model topology, as shown in Fig. 3. Such an approach makes it easier for us to map unavailable geometrical details in the clinical imaging routine (e.g. cardiac myofiber architecture or the geometrical Purkinje network) from one model to another. By mapping relevant anatomical landmarks from the baseline model to various subject-specific hearts, our approach also enables systematic quantitative descriptions of anatomical variability within a specific patient population.

Accuracy. Our local geometric accuracy studies, shown in Table 1, show an average Dice Similarity Coefficient ranging from 0.681 to 0.830. This demonstrates that our approach generated geometric models with good spatial agreement (DSC > 0.70 [23]) with the segmented MR images. Current state-of-the-art deep learning cardiac image segmentation approaches have reached biventricular segmentation (differentiating tissue and blood volumes) Dice scores ranging between 0.780 and 0.950 [5]. However, these approaches worked with vast amounts of ground-truth image segmentations for healthy adults to train these networks. For the more challenging young CHD populations, we did not find any works reporting Dice scores with respect to deep learning based myocardial tissue segmentation accuracy. For relatively easier segmentation of left and

right ventricular blood volume, state-of-the-art approaches achieved Dice scores ranging between 0.537 and 0.906 in a young CHD population [7].

Slice Shift Correction. We demonstrated the validity of two strategies to correct for slice shift misalignment in the original short-axis image stack. Based on our analysis of the healthy patient with the greatest slice shift, we found that the papillary-muscle based re-centering approach provided slightly better results than the LV center of mass re-centering approach. However, it is important to note that this conclusion is limited by the absence of long-axis image slices for the other patients, which prevented us from conducting a systematic evaluation across the entire pediatric CHD patient population. If these long-axis slices were available, a multi-view loss objective function could be incorporated to automate the slice shift correction [20], and quantify the validity of our two approaches. Working only with short-axis image slices, another potential solution would be to incorporate an additional anatomic landmark, such as the spine, into the imaged region of interest, and use this landmark for realignment. In our case, such a landmark unfortunately fell outside the imaged region of interest.

Manual Work. Our proof-of-concept framework involves a substantial amount of manual morphing work, where we iteratively tune global dimensions (global scaling), update the translation and rotation vector (global alignment), modify the LV and RV shape parameters (parametric morphing), and finally locally sculpt the endocardial and epicardial surfaces (manual morphing). To a trained fellow, these steps easily take a few hours per subject-specific heart. As such, we aim to automate the global alignment, scaling and parametric morphing steps in our framework. With this goal in mind, we envision our approach can greatly benefit from – but also provide greater flexibility to – statistical shape modeling techniques [3,10,18,22]. On the one hand, statistical shape modeling techniques can automate some steps in our shape morphing framework [14]. On the other hand, the flexibility of our final manual morphing allows us to create more subject-specific heart models that are potentially not represented by statistical shape models trained on limited pediatric CHD imaging datasets [1]. Additionally, we currently started from a healthy human heart as a high-fidelity starting point. In the future, we aim to collect CHD-specific medical imaging data with a higher spatial resolution that allows the development of CHD phenotype-specific high-fidelity heart models to start the shape morphing process from.

Note

This chapter is a summary of the MSc graduation project conducted by Puck Pentenga (AY 2022–2023) at Delft University of Technology. A more detailed description of this work and the developed population of CHD-image-informed biventricular CAD model geometry files can be found on the TU Delft MSc Thesis repository.

References

1. Albà, X., et al.: Reusability of statistical shape models for the segmentation of severely abnormal hearts. In: Camara, O., Mansi, T., Pop, M., Rhode, K., Sermesant, M., Young, A. (eds.) STACOM 2014. LNCS, vol. 8896, pp. 257–264. Springer, Cham (2015). https://doi.org/10.1007/978-3-319-14678-2_27

2. Babu-Narayan, S.V., Giannakoulas, G., Valente, A.M., Li, W., Gatzoulis, M.A.: Imaging of congenital heart disease in adults. Eur. Heart J. **37**(15), 1182–1195 (2015). https://doi.org/10.1093/eurheartj/ehv519

3. Bai, W., et al.: A bi-ventricular cardiac atlas built from 1000+ high resolution MR images of healthy subjects and an analysis of shape and motion. Med. Image Anal. **26**(1), 133–145 (2015). https://doi.org/10.1016/j.media.2015.08.009

4. Biglino, G., Capelli, C., Bruse, J., Bosi, G.M., Taylor, A.M., Schievano, S.: Computational modelling for congenital heart disease: how far are we from clinical translation? Heart **103**(2), 98–103 (2016). https://doi.org/10.1136/heartjnl-2016-310423

5. Chen, C., et al.: Deep learning for cardiac image segmentation: a review. Front. Cardiovasc. Med. **7** (2020). https://doi.org/10.3389/fcvm.2020.00025

6. Gilbert, K., Cowan, B.R., Suinesiaputra, A., Occleshaw, C., Young, A.A.: Rapid D-affine biventricular cardiac function with polar prediction. In: Golland, P., Hata, N., Barillot, C., Hornegger, J., Howe, R. (eds.) MICCAI 2014. LNCS, vol. 8674, pp. 546–553. Springer, Cham (2014). https://doi.org/10.1007/978-3-319-10470-6_68

7. Karimi-Bidhendi, S., Arafati, A., Cheng, A.L., Wu, Y., Kheradvar, A., Jafarkhani, H.: Fully-automated deep-learning segmentation of pediatric cardiovascular magnetic resonance of patients with complex congenital heart diseases. J. Cardiovasc. Magn. Resonance **22**(1) (2020). https://doi.org/10.1186/s12968-020-00678-0

8. Levine, S., Battisti, T., Butz, B., D'Souza, K., Costabal, F.S., Peirlinck, M.: Dassault systèmes' living heart project. In: Modelling Congenital Heart Disease, pp. 245–259. Springer International Publishing, Cham (2022). https://doi.org/10.1007/978-3-030-88892-3_25

9. van der Linde, D., et al.: Birth prevalence of congenital heart disease worldwide. J. Am. Coll. Cardiol. **58**(21), 2241–2247 (2011). https://doi.org/10.1016/j.jacc.2011.08.025

10. Marciniak, M., et al.: A three-dimensional atlas of child's cardiac anatomy and the unique morphological alterations associated with obesity. Eur. Heart J. Cardiovasc. Imaging **23**(12), 1645–1653 (2021). https://doi.org/10.1093/ehjci/jeab271

11. Mitchell, F.M.: Cardiovascular magnetic resonance: diagnostic utility and specific considerations in the pediatric population. World J. Clin. Pediatr. **5**(1), 1 (2016). https://doi.org/10.5409/wjcp.v5.i1.1

12. Naci, H., et al.: Impact of predictive medicine on therapeutic decision making: a randomized controlled trial in congenital heart disease. NPJ Digit. Med. **2**(1) (2019). https://doi.org/10.1038/s41746-019-0085-1

13. Niederer, S.A., Lumens, J., Trayanova, N.A.: Computational models in cardiology. Nat. Rev. Cardiol. **16**(2), 100–111 (2018). https://doi.org/10.1038/s41569-018-0104-y

14. Ordas, S., Oubel, E., Leta, R., Carreras, F., Frangi, A.F.: A statistical shape model of the heart and its application to model-based segmentation. In: Manduca, A., Hu, X.P. (eds.) SPIE Proceedings. SPIE, March 2007. https://doi.org/10.1117/12.708879

15. Peirlinck, M., et al.: Flow optimization in the reconstructed hypoplastic aortic arch. In: Proceedings of the 5th International Conference on Engineering Frontiers in Pediatric and Congenital Heart Disease, pp. 76–78 (2016)

16. Peirlinck, M., et al.: Precision medicine in human heart modeling. Biomech. Model. Mechanobiol. **20**(3), 803–831 (2021). https://doi.org/10.1007/s10237-021-01421-z

17. Peirlinck, M., et al.: Kinematic boundary conditions substantially impact in silico ventricular function. Int. J. Numer. Methods Biomed. Eng. **35**(1), e3151 (2018). https://doi.org/10.1002/cnm.3151

18. Rodero, C., et al.: Linking statistical shape models and simulated function in the healthy adult human heart. PLOS Comput. Biol. **17**(4), e1008851 (2021). https://doi.org/10.1371/journal.pcbi.1008851

19. Tikenoğulları, O.Z., Peirlinck, M., Chubb, H., Dubin, A.M., Kuhl, E., Marsden, A.L.: Effects of cardiac growth on electrical dyssynchrony in the single ventricle patient. Comput. Methods Biomech. Biomed. Eng. (2023). https://doi.org/10.1080/10255842.2023.2222203

20. Wang, S., et al.: Joint motion correction and super resolution for cardiac segmentation via latent optimisation. In: de Bruijne, M., et al. (eds.) MICCAI 2021. LNCS, vol. 12903, pp. 14–24. Springer, Cham (2021). https://doi.org/10.1007/978-3-030-87199-4_2

21. Weissmann, J., Charles, C.J., Richards, A.M., Yap, C.H., Marom, G.: Cardiac mesh morphing method for finite element modeling of heart failure with preserved ejection fraction. J. Mech. Behav. Biomed. Mater. **126**, 104937 (2022). https://doi.org/10.1016/j.jmbbm.2021.104937

22. Young, A.A., Frangi, A.F.: Computational cardiac atlases: from patient to population and back. Exp. Physiol. **94**(5), 578–596 (2009). https://doi.org/10.1113/expphysiol.2008.044081

23. Zou, K.H., et al.: Statistical validation of image segmentation quality based on a spatial overlap index1. Acad. Radiol. **11**(2), 178–189 (2004). https://doi.org/10.1016/s1076-6332(03)00671-8

24. Zygote Media Group Inc: Zygote solid 3d human anatomy - generation ii - development report. Technical report (2014). https://www.zygote.com